Superfluid ^{4}He dynamics beyond quasiparticle excitations

K. Beauvois,[1,2,3] C. E. Campbell,[4] J. Dawidowski,[5] B. Fåk,[1,6,7] H. Godfrin,[2,3,*] E. Krotscheck,[8,9] H.-J. Lauter,[10] T. Lichtenegger,[8,9] J. Ollivier,[1] and A. Sultan[2,3,7]

[1]*Institut Laue-Langevin, 6, rue Jules Horowitz, 38042 Grenoble, France*
[2]*Université Grenoble Alpes, Institut NEEL, F-38000 Grenoble, France*
[3]*CNRS, Institut NEEL, F-38042 Grenoble, France*
[4]*School of Physics and Astronomy, University of Minnesota, Minneapolis, Minnesota 55455, USA*
[5]*Comisión Nacional de Energía Atómica and CONICET, Centro Atómico Bariloche, (8400) San Carlos de Bariloche, Río Negro, Argentina*
[6]*Université Grenoble Alpes, INAC-SPSMS, F-38000 Grenoble, France*
[7]*CEA, INAC-SPSMS, F-38000 Grenoble, France*
[8]*Department of Physics, University at Buffalo, SUNY Buffalo, New York 14260, USA*
[9]*Institute for Theoretical Physics, Johannes Kepler University, A-4040 Linz, Austria*
[10]*Spallation Neutron Source, Oak Ridge National Laboratory, Oak Ridge, Tennessee 37831, USA*

(Received 17 March 2016; revised manuscript received 5 May 2016; published 11 July 2016)

The dynamics of superfluid ^{4}He at and above the Landau quasiparticle regime is investigated by high-precision inelastic neutron scattering measurements of the dynamic structure factor. A highly structured response is observed above the familiar phonon-maxon-roton spectrum, characterized by sharp thresholds for phonon-phonon, maxon-roton, and roton-roton coupling processes. The experimental dynamic structure factor is compared to the calculation of the *same* physical quantity by a dynamic many-body theory including three-phonon processes self-consistently. The theory is found to provide a quantitative description of the dynamics of the correlated bosons for energies up to about three times that of the Landau quasiparticles.

DOI: 10.1103/PhysRevB.94.024504

I. INTRODUCTION

Liquid ^{4}He is the prime example of a strongly correlated quantum many-body system. It has been studied for decades and still offers surprises that lead to new insights. Understanding the helium fluids, due to their generic nature, lies at the core of understanding other strongly correlated many-particle systems and is therefore of interest to more than the quantum fluids community. The description of the elementary excitations of superfluid ^{4}He in terms of phonon-roton quasiparticles is a cornerstone of modern physics, with profound implications in condensed-matter physics, particle physics, and cosmology. The empirical dispersion relation of these excitations proposed by Landau [1,2] to explain thermodynamic data found support in the microscopic theory of Feynman and Cohen [3], initiating a fruitful development of the field-theoretic description of correlated quantum particles.

From an experimental point of view, neutron scattering techniques allowed direct observation of very sharp excitations in superfluid ^{4}He at low temperatures. The density fluctuations displayed, as predicted, a continuous phonon-maxon-roton dispersion curve: a linear phonon part at low wave vectors followed by a maximum ("maxon") and then a pronounced "roton" minimum at a finite wave vector of atomic dimensions. Phonons naturally arise as the Goldstone mode associated with the continuous symmetry of the interacting system, whereas rotons are a direct consequence of strong correlations. Rotonlike excitations have been proposed in cold atomic gases [4], in one-dimensional ^{4}He [5], and in two-dimensional fermionic systems [6]. Superfluidity emerges phenomenologically as a natural consequence of the dynamics, while the knowledge of the dispersion relation allows the calculation of low-temperature thermodynamic properties of superfluid ^{4}He [7].

The relation between theory and experiment, however, is not straightforward [8,9]. The excitations considered by Landau, Feynman, and others correspond to the single-particle response function associated with the description of an effective vacuum (the superfluid ground state) and noninteracting quasiparticle excitations. Neutron scattering, in turn, gives access to the dynamic structure factor $S(Q,\omega)$, a quantity related to the dynamic susceptibility, i.e., the linear response of the system to a density fluctuation. The latter has a strong weight along the phonon-roton dispersion curve, but it also contains additional contributions, already observed in early neutron scattering experiments [10–13]. Much of the work on superfluid ^{4}He has been focused on the single-particle response function, attempting to extract the quasiparticle dispersion relation [12] and lifetime [14,15] from neutron data. In parallel, considerable effort has been devoted to the development of an accurate theoretical description of the dynamics of superfluid ^{4}He using various techniques [9,16–20].

In this paper, we investigate in detail the multiexcitation region of the dynamic structure factor $S(Q,\omega)$ of superfluid ^{4}He. We present high-precision neutron scattering measurements of $S(Q,\omega)$ at very low temperatures. We find several unique features, in particular a "ghost phonon," and also multiparticle thresholds that are much sharper than in earlier experimental work. These features are in agreement with a quantitative microscopic calculation of the density fluctuations $S(Q,\omega)$ within a recent dynamic many-body theory [20]. Theoretical and experimental results for $S(Q,\omega)$ in a broad sector of the spectrum can be compared directly, leading to

*henri.godfrin@neel.cnrs.fr

an unprecedentedly accurate description of the dynamics of superfluid ^{4}He.

II. NEUTRON SCATTERING MEASUREMENTS

The inelastic neutron scattering measurements were performed on the neutron time-of-flight spectrometer IN5 at the Institut Laue-Langevin using an incoming energy of 3.55 meV (wavelength 4.8 Å) and an energy resolution at elastic energy transfer of 0.07 meV. The high-purity superfluid ^{4}He sample was contained in a thin-walled cylindrical aluminum container of inner diameter 15 mm. The effective sample height in the beam was 50 mm. Cadmium disks were placed inside the cell at intervals of 10 mm to reduce multiple scattering, an important experimental artifact discussed below. The cell was connected to the mixing chamber of a dilution refrigerator via a copper piece equipped with silver sinter to ensure good thermal contact, thereby allowing measurements to be done at very low temperatures, $T < 100$ mK. The measurements were performed at saturated vapor pressure.

The quantity measured by a neutron spectrometer, the inelastic differential scattering cross section per target atom, is proportional to the dynamic structure factor:

$$\frac{\partial^2\sigma}{\partial\Omega\partial\hbar\omega} = \frac{b_c^2}{\hbar}\frac{k'}{k}S(Q,\omega),$$

where b_c is the bound-atom coherent scattering length, k and k' are the neutron wave vectors before and after the scattering process, Q is the wave vector transfer, and $\hbar\omega$ is the energy transfer [9]. Standard data reduction routines [21] were used to obtain the dynamic structure factor from the neutron raw spectra. The magnitude of $S(Q,\omega)$ was normalized by requiring that the single quasiparticle strength $Z(Q) = 0.93$ for $Q = 2.0$ Å^{-1}, a value obtained from previous works [9,10,20]. Figure 1(a) displays essentially the raw data, after the usual corrections. The aluminum-cell elastic background, measured before introducing the helium in the cell, was subtracted from the raw spectra. This led to the noisy region seen in Fig. 1(a) near zero energy. We also subtracted the inelastic signal originating from scattering events involving the aluminum cell and the helium sample. Rotons, due to their high density of states, dominate these processes, and this contribution is only significant at the roton energy. Since it is essentially Q independent, it can be easily identified and removed. The subtraction of this contribution spoils the accuracy of the data in a small range around the roton energy in regions of the spectrum where the signal is small. The effect can be seen if the intensity scale is considerably expanded, for instance, as in Fig. 2.

While earlier neutron scattering experiments [10–13] revealed the presence of broad, rather featureless multiparticle excitation regions above the single-particle dispersion curve, the improved precision (and possibly the much lower temperature) in the present experiment allowed us to observe a very rich structure in this region, with increasing weight at large wave vectors, as seen in the measured $S(Q,\omega)$ shown in Fig. 1(a).

It is particularly important to distinguish the multiparticle excitations under investigation, which are an intrinsic property of helium, from multiple scattering. The former arise when a neutron creates in a single process a high-energy perturbation

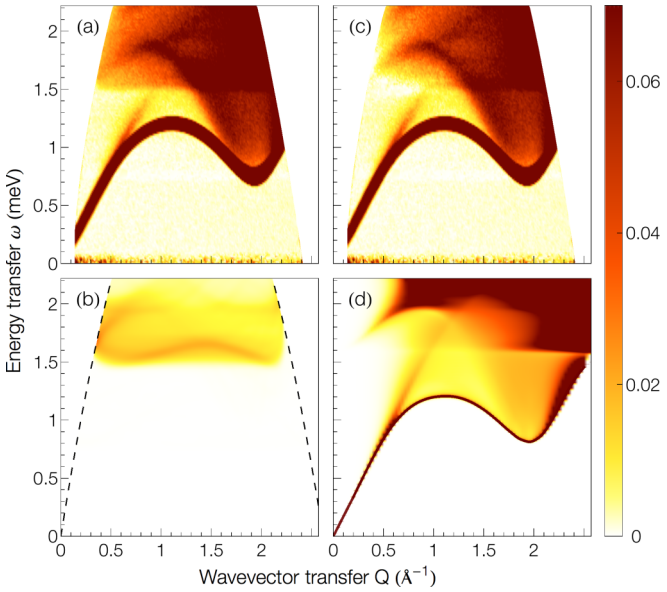

FIG. 1. (a) $S(Q,\omega)$ of superfluid ^{4}He measured as a function of wave vector and energy transfer at saturated vapor pressure and temperature $T \leqslant 100$ mK. Contributions involving scattering with the aluminum cell have been subtracted but not multiple scattering within the helium. (b) Helium multiple-scattering contribution (numerical simulation); note that its magnitude is comparable to the multiparticle intensity seen in (c) and (d) and in Fig. 3. The dashed lines show the limits of the instrumental range, also valid for (a) and (c). (c) Experimental dynamic structure factor $S(Q,\omega)$ after correction for multiple scattering. (d) Dynamic many-body theory calculation of $S(Q,\omega)$. Note that all the detailed features of the experimental data are reproduced. The units of the contour-plot scale are meV^{-1}. The intensity is cut off at 0.07 meV^{-1} in order to emphasize the multiexcitation region. The apparent width of the Landau excitations in the experimental plot is due to the experimental resolution of 0.07 meV, while the calculated Landau dispersion curve has been highlighted by a thick line.

which can decay into two or more excitations, while the latter is a spurious effect, dependent on the sample size, where a single neutron creates two or more excitations in successive scattering events. Since the two kinds of processes fulfill the same kinematic conservation rules and their contributions have similar intensity for typical sample sizes, subtracting multiple scattering from the raw data is essential when dealing with the multiparticle region of the spectrum.

It is difficult in practice to determine this contribution experimentally [22], for instance, by using samples of different diameters, as one could naively believe. For this reason, we instead chose to perform an accurate calculation of the multiple-scattering contribution using simulation software [23], and we verified the results with two other simulation programs [24,25]. All three Monte Carlo programs track successive neutrons in a sample of given geometrical and physical characteristics, in particular its scattering function $S(Q,\omega)$. They have been adapted to calculate multiple scattering in helium. This contribution, shown in Fig. 1(b), is found to be of the same order of magnitude as multiparticle excitations in all the region above 1.5 meV. The ratio of the multiple-scattering intensity over the total intensity is 1.8%, a value in agreement with

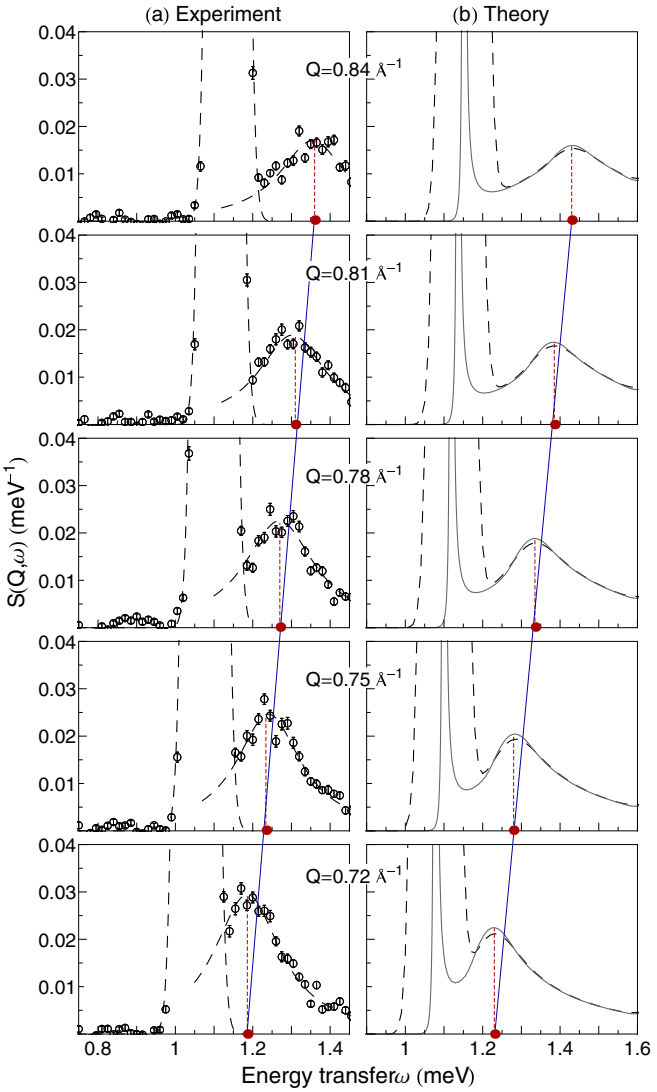

FIG. 2. (a) Experimental dynamic structure factor $S(Q,\omega)$: spectra at different wave vectors Q in the phonon region. The dashed lines are Gaussian fits of the phonon peak (cut off) and the much smaller "ghost phonon." The maxima of the ghost phonon, indicated by vertical dashed lines, are located on the linear extension of the phonon dispersion (solid line). (b) Calculated spectra before and after convolution with the experimental resolution of 0.07 meV, shown as solid and dashed lines, respectively. The experimental data are very well reproduced by the mode-mode coupling calculation.

the calculation using the well-known semianalytical method developed by Sears [22]. Multiple scattering was subtracted from the raw data, leading to the corrected results for $S(Q,\omega)$ shown in Fig. 1(c). The results shown in the figures clearly demonstrate that the unique features we observe in this work are *not* caused by a multiple-scattering artifact.

Having obtained reliable data for the multiparticle region of $S(Q,\omega)$, we can claim the unambiguous experimental observation of three new features in $S(Q,\omega)$: (i) a feature that we have named *ghost phonon* for obvious reasons since it appears as scattering strength extrapolating linearly from the phonon for wave vectors $0.6 < Q < 0.9$ Å^{-1}, (ii) a prominent branchlike feature that appears at about twice the maxon energy, and (iii) a sharp *threshold* at twice the roton energy that extends to low wave vectors. Previous experimental works, including ours, show traces of the second feature at the limit of the experimental resolution. Comparing the plots of Refs. [10–13] with the results shown in Fig. 1(c) illustrates the magnitude of the improvement in neutron techniques over the last decade.

III. DYNAMIC MANY-BODY CALCULATIONS

The kinematic possibility of the decay of a mode into two low-lying quasiparticle excitations under energy and momentum conservation is a necessary condition for these effects to occur, and the observed features can be ascribed to modes decaying into pairs of excitations of large spectral weight. Even in the absence of a theory, it is possible to combine pairs of single-particle excitations to obtain the *position* of the main multiexcitation resonances in the dynamic structure factor (two-phonon, two-roton, two-maxon, and maxon-roton resonances). We observe, however, that obtaining the fine structure requires a quantitative calculation of mode couplings. Theoretical calculations [26,27] based on early versions of the CBF (correlated basis function) method gave a highly structured multiexcitation region in the dynamic structure factor, which at first sight looks similar to the present experimental results. The similarity does not stand up to a more thorough inspection since even the single-particle modes were only very qualitatively reproduced. In particular, the calculated multiexcitations decay into Feynman modes instead of the true single-particle excitations, leaving large gaps in the spectrum. Also, the calculations predicted several additional features at high energies that have not been found in experiments. They provided, nevertheless, an appealing example of the effects that could be expected and hence a motivation for further investigation of multiparticle dynamics.

The challenge to the theory imposed by the present data was to obtain the magnitudes of the corresponding coupling matrix elements. They have been calculated in this work using dynamic many-body theory [20,28], which can describe excitations with wavelengths comparable to the interparticle distance. This requires an appropriate treatment of correlations at atomic scales. In their pioneering work, Feynman and Cohen introduced pair fluctuations [3], which allowed them to take into account "backflow" effects. In order to calculate mode-mode couplings in a microscopic and quantitative manner, we include here n-particle fluctuations for all n.

The dynamic structure factor calculated for a number density of $\rho = 0.022$ Å^{-3} is shown in Fig. 1(d). It is in quite satisfactory agreement with the experimental data. In addition to the well-known features of superfluid ^{4}He, namely, the linear phonon dispersion relation, the maxon, and the roton part of the spectrum turning eventually into the Pitaevskii plateau [29], the calculated $S(Q,\omega)$ also shows the finer features revealed by our high-precision experiment [see Fig. 1(c)].

Our dynamic many-body calculations predict a ghost phonon which, as seen in Fig. 1, extends to about twice the wave vector up to which the dispersion relation is essentially linear. This can be shown explicitly by the calculation of the three-phonon interaction [20]. Figure 2 shows that the energy, strength, and shape of the calculated ghost phonon agree very

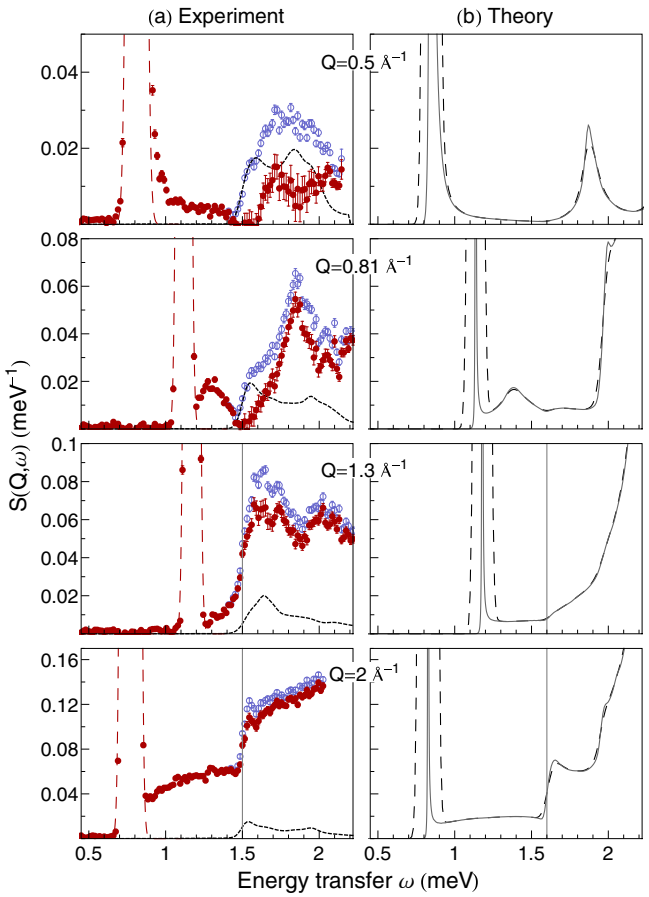

FIG. 3. (a) Experimental dynamic structure factor $S(Q,\omega)$: spectra for different wave vectors Q. Open circles: raw data; short-dashed line: calculated multiple-scattering contribution; solid circles: $S(Q,\omega)$ corrected data (see text). The dashed lines are Gaussian fits of the phonon-roton peaks (cut off). (b) Theoretical dynamic structure factor spectra for the same wave vectors Q before and after convolution with the experimental resolution of 0.07 meV, shown as solid and dashed lines, respectively. The plots have been chosen to emphasize differences between theory and experiment not readily observable in Fig. 1. Thin vertical lines: roton-roton threshold.

well with the experiment, even for wave vectors at atomic scale, of the order of 1 Å^{-1}.

The mode above the maxon stems from interactions between rotons and maxons. Modes with that frequency and a wave vector close to that of the maxon decay predominantly into maxon and roton excitations with momenta close to those of rotons and maxons but directed parallel and antiparallel to the initial wave vector, respectively. A discussion of the kinematic situation, estimated by approximating the dispersion relation in the maxon and roton regions, is given in Ref. [20]. This feature is clearly present both in the experiments and the theory, and Figs. 1(c) and 1(d) are very similar for energies as high as 2 meV.

A more quantitative comparison can be made on the spectra shown in Fig. 3. The experimental spectrum at $Q = 0.5$ Å^{-1} is indeed very close to its theoretical analog. At higher wave vectors, $Q = 0.8$ Å^{-1}, however, it is clear that only the low-energy side of the experimental feature is reproduced by the theory. Contrary to the situation encountered in the phonon region, where a very detailed calculation could be made, here the number of possible intermediate channels renders the calculation particularly demanding. The obtained semiquantitative agreement is already quite gratifying.

The decay of an excitation of energy $2\Delta_r$ into two rotons with increasing angle between them explains the plateau or threshold that we observe down to low wave vectors. The effect, which has been extensively investigated [29], is discussed in detail in Ref. [20]. The noteworthy observation is that this structure is observable, with comparable strength in both experiments and theory (see Fig. 3), even below the maxon wave vector.

IV. CONCLUSIONS

In conclusion, the dynamic structure factor of superfluid ^{4}He, a canonical model system for correlated boson physics, exhibits a rich behavior at intermediate energies. We observe thresholds and fine structures delimited by kinematic constraints. The results are in remarkable agreement with the microscopic dynamic many-body calculation. There are still some quantitative differences, observable above the roton energy for wave vectors smaller than the roton one, between 1 and 2 Å^{-1}. The experiments display a sizable response, which is present but weaker in the theory, as seen in Figs. 1 and 3. The origin of the observed enhancement of this interesting mode remains an open question for theorists. There are also undeniable discrepancies with the theory at energies above 2 meV. These can, however, be easily ascribed to higher-order processes [20]; they are mostly structureless and do not lend themselves to a clear identification. The combined experimental and theoretical work reported herein represents significant progress in the understanding of the effects of correlations on the dynamics of quantum fluids.

ACKNOWLEDGMENTS

We are grateful to X. Tonon for his help with the experiment, and to E. Farhi for his help with the program McStas. This work was supported, in part, by the Austrian Science Fund FWF grant I602, the French grant ANR-2010-INTB-403-01 and the European Community Research Infrastructures under the FP7 Capacities Specific Programme, MICROKELVIN Project No. 228464.

[1] L. D. Landau, J. Phys. (Moscow) **5**, 71 (1941).
[2] L. D. Landau, J. Phys. (Moscow) **11**, 91 (1947).
[3] R. P. Feynman and M. Cohen, Phys. Rev. **102**, 1189 (1956).
[4] A. Macia, D. Hufnagl, F. Mazzanti, J. Boronat, and R. E. Zillich, Phys. Rev. Lett. **109**, 235307 (2012).
[5] G. Bertaina, M. Motta, M. Rossi, E. Vitali, and D. E. Galli, Phys. Rev. Lett. **116**, 135302 (2016).

[6] H. Godfrin, M. Meschke, H.-J. Lauter, A. Sultan, H. M. Böhm, E. Krotscheck, and M. Panholzer, Nature (London) **483**, 576 (2012).
[7] R. J. Donnelly, J. A. Donnelly, and R. N. Hills, J. Low Temp. Phys. **44**, 471 (1981).
[8] D. Pines and P. Nozières, *The Theory of Quantum Liquids* (Addison-Wesley, Redwood City, CA, 1990), Vol. 1.
[9] H. R. Glyde, *Excitations in Liquid and Solid Helium* (Clarendon, Oxford, 1994).
[10] R. A. Cowley and A. D. B. Woods, Can. J. Phys. **49**, 177 (1971).
[11] K. H. Andersen, W. G. Stirling, R. Scherm, A. Stunault, B. Fåk, H. Godfrin, and A. J. Dianoux, Phys. B: Condensed Matter **180-181**, 851 (1992).
[12] K. H. Andersen, W. G. Stirling, R. Scherm, A. Stunault, B. Fåk, H. Godfrin, and A. J. Dianoux, J. Phys. Condens. Matter **6**, 821 (1994).
[13] M. R. Gibbs, K. H. Andersen, W. G. Stirling, and H. Schober, J. Phys. Condens. Matter **11**, 603 (1999).
[14] F. Mezei, Phys. Rev. Lett. **44**, 1601 (1980).
[15] B. Fåk, T. Keller, M. E. Zhitomirsky, and A. L. Chernyshev, Phys. Rev. Lett. **109**, 155305 (2012).
[16] *Introduction to Modern Methods of Quantum Many-Body Theory and Their Applications*, edited by A. Fabrocini, S. Fantoni, and E. Krotscheck, Advances in Quantum Many-Body Theory Vol. 7 (World Scientific, Singapore, 2002).
[17] S. Moroni, D. E. Galli, S. Fantoni, and L. Reatto, Phys. Rev. B **58**, 909 (1998).
[18] E. Vitali, M. Rossi, L. Reatto, and D. E. Galli, Phys. Rev. B **82**, 174510 (2010).
[19] F. Arrigoni, E. Vitali, D. E. Galli, and L. Reatto, Fiz. Nizk. Temp. (Kiev) **39**, 1021 (2013) [Low Temp. Phys. **39**, 793 (2013)] .
[20] C. E. Campbell, E. Krotscheck, and T. Lichtenegger, Phys. Rev. B **91**, 184510 (2015).
[21] LAMP (Large Array Manipulation Program), http://www.ill.eu/data_treat/lamp.
[22] V. F. Sears, Adv. Phys. **24**, 1 (1975).
[23] J. Dawidowski, F. J. Bermejo, and J. R. Granada, Phys. Rev. B **58**, 706 (1998).
[24] K. Lefmann and K. Nielsen, Neutron News **10**, 20 (1999).
[25] J. R. D. Copley, P. Verkerk, A. A. van Well, and H. Fredrikze, Comput. Phys. Commun. **40**, 337 (1986).
[26] M. Saarela, in *Introduction to Modern Methods of Quantum Many-Body Theory and Their Applications* (Ref. [16]), pp. 205–264.
[27] M. Saarela, Phys. Rev. B **33**, 4596 (1986).
[28] C. E. Campbell and E. Krotscheck, Phys. Rev. B **80**, 174501 (2009).
[29] L. P. Pitaevskii, Zh. Eksp. Teor. Fiz. **36**, 1168 (1959) [Sov. Phys. JETP **9**, 830 (1959)].